Available online at www.sciencedirect.com
SCIENCE DIRECT®
Thermochimica Acta 428 (2005) 57–62
thermochimica acta
www.elsevier.com/locate/tca

Effect of pressure on phase behavior of a thermotropic cubic mesogen

Yoji Maeda[a,*], Teruki Niori[b], Jun Yamamoto[b], Hiroshi Yokoyama[a,b]

[a] *Nanotechnology Research Institute, National Institute of Advanced Industrial Science and Technology, Higashi 1-1, Tsukuba, Ibaraki 305-8565, Japan*
[b] *Yokoyama Nano-Structured Liquid Crystal Project, JST, Tsukuba, Ibaraki 300-2635, Japan*

Received 9 May 2004; received in revised form 23 September 2004; accepted 27 September 2004

Abstract

The phase behavior of an optically isotropic, thermotropic cubic mesogen 4-(ethylpentoxy)-anilinebenzylidenen-4′-carboxylic acid was investigated under pressures up to 300 MPa using a high-pressure differential thermal analyzer, a wide-angle X-ray diffractometer (WAXD) and a polarizing optical microscope (POM) equipped with a high-pressure optical cell. The cubic phase was found in the whole pressure region, although its temperature region decreased gradually with increasing pressure. The phase transition sequence, crystal (Cr)–cubic (Cub)–isotropic liquid (I) observed at atmospheric pressure, is held under pressures, while a high-temperature crystal polymorph appears under elevated pressures above about 160 MPa.

Keywords: Thermotropic cubic mesogen; High-pressure DTA; Phase sequence; *T* versus *P* phase diagram; Pressure-induced crystal polymorph

1. Introduction

Study on optically isotropic, thermotropic cubic mesogen started in 1957, when Gray et al. [1] reported the synthesis of 4′-*n*-hexadecyloxy- and 4′-*n*-octadecyloxy-3′-nitrobiphenyl-4-carboxylic acid: referred to as ANBC(16) and ANBC(18), respectively. Since then, a number of thermotropic cubic mesogens have now been reported [2]. The majority of these compounds are carbohydrates and polycatenar compounds including several metalomesogens. The cubic phases for ANBC(16) and ANBC(18) are known to have the structure with *Ia*3*d* space group. The jointed-rod model for the cubic phase with *Ia*3*d* space group, i.e. two interwoven, but unconnected networks of rods linked three by three [3–6], is suggested.

Although many researches into the phase transition behavior of the thermotropic cubic mesogens have been performed, there are only a few studies on the high-pressure investigation of the cubic phases [7–13]. One of the authors (Y.M.) reported the interesting phase behavior of ANBC(16) [8,9], ANBC(20) and ANBC(22) [10], and 1,2-bis(4-*n*-alkyloxybenzoyl)hydrazine (BABH(*n*) with carbon number *n* of methylene groups in the alkoxy chain, $n = 8$, 10–12 [11–13] under hydrostatic pressure. ANBC(*n*)s having the methylene groups of $n = 16$–22 show generally the phase transition sequence of crystal (Cr)–smectic C (SmC)–cubic (Cub)–(SmA for $n = 16$)–isotropic liquid (I), where BABH(*n*)s having the methylene groups of $n = 8$–10 exhibit the Cr–Cub–SmC–I transition sequence. The phase order between the SmC and cubic phases is inversed in the BABH(*n*) system. The *T* versus *P* phase diagrams of ANBC(*n*) system show that the SmC–Cub transition line has positive values for slope (d*T*/d*P*), but the phase diagrams of BABH(8) and BABH(10) exhibit that the Cub–SmC transition lines have negative slopes. The triple point for the Cr, Cub and SmC phases is found at very low pressures in BABH(8) and BABH(10), indicating the upper limit of pressure for the cubic phase formation. Also, in the ANBC(*n*), the cubic phase is destabilized with increasing pressure be-

* Corresponding author. Tel.: +81 29 861 6282; fax: +81 29 861 6282.
E-mail address: yoji.maeda@aist.go.jp (Y. Maeda).

0040-6031/$ – see front matter © 2004 Elsevier B.V. All rights reserved.
doi:10.1016/j.tca.2004.09.030

cause the temperature range decreases with increasing pressure.

On the other hand, racemic 4-(ethylpentoxy)-anilinebenzylidene-4′-carboxylic acid, abbreviated as EPABC, shows an optically isotropic cubic phase between the crystalline and isotropic liquid phases. This system exhibits reversibly a simple transition sequence of Cr–Cub–I under atmospheric pressure [14]. The chemical structure of EPABC is shown below.

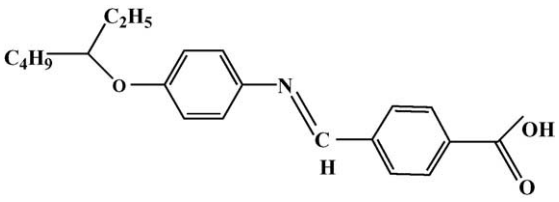

This molecule has a anilinebenzylidene group as a central core, and ethylpentoxy group as a flexible spacer. Since EPABC molecule has a carboxylic acid group at a molecular end such as ANBC(*n*) system, the molecules form a dimerized structural unit in the crystal and mesophae through hydrogen bonding between the carboxylic acid groups of neighboring molecules. The dimerized molecule has the anilinebenzylidene carboxylic acid dimer as a central core and two ethylpentoxy groups as a flexible spacer. The dimerized molecule here may have a molecular shape of polycatenar compound with a short arm at both ends.

The interesting phase behavior of the cubic phase for ANBC(16) and BABH(8) under pressure prompted us to continue the study on phase behavior of various cubic mesogens under hydrostatic pressure, particularly focused on the effect of pressure on the phase stability of cubic phase. In this paper, we present the experimental results of the effect of pressure on the thermal, morphological and structural behavior of EPABC under hydrostatic pressures up to 300 MPa using a high-pressure DTA, a wide-angle X-ray diffractometer (WAXD) and a polarizing optical microscope (POM) equipped with a high-pressure optical cell.

2. Experimental

2.1. Sample characterization

The EPABC sample used in this study is described in elsewhere [14]. Thermal characterization was performed on a Perkin-Elmer DSC-7 differential scanning calorimeter at a scanning rate of 5 °C min^{-1} under N_2 gas flow. Transition temperature and heat of transition were calibrated using the standard materials (indium and tin). Transition temperatures were determined as the onset of the transition peaks at which the tangential line of the inflection point of the rising part of the peak crosses over the extrapolated baseline. Texture observation was performed using a Leiz Orthoplan polarizing optical microscope (POM) equipped with a Mettler hot stage FP-82.

2.2. DTA measurements under pressure

The high-pressure DTA apparatus used in this study is described elsewhere [15]. The DTA system was operated in a temperature region between room temperature and 250 °C under hydrostatic pressures up to 300 MPa. Dimethylsilicone oil with a medium viscosity (1×10^{-4} m^2/s) was used as the pressurizing medium. The sample weighing about 4 mg was put in the sample cell and coated with epoxy adhesives, to fix the sample at the bottom of the cell and also to prevent direct contact with the silicone oil. New specimen of EPABC was used for each DTA measurement. The DTA runs were performed at a constant heating rate of 5 °C min^{-1} under various pressures. Peak temperatures were adopted as transition temperatures for making the temperature versus pressure phase diagram.

2.3. Morphological and X-ray characterization under pressure

The morphological texture of the sample under hydrostatic pressure was observed using a Leitz Orthoplan POM equipped with a high-pressure optical cell [16]. The texture observation was performed on heating process at 60 and 100 MPa.

The X-ray diffraction patterns of the sample under pressure were obtained using the high-pressure wide-angle X-ray diffraction apparatus [15]. The high-pressure vessel was set on the wide-angle goniometer of a 12 kW rotating anode type of X-ray generator (Rotaflex RU200, Rigaku Co.). The sample was inserted into the vertical hole of the beryllium spindle as the sample cell. The beryllium spindle was mechanically compressed for pressure sealing using upper and lower pressure blocks. Then the sample was pressurized hydrostatically at pressures up to 200 MPa. A Ni-filtered Cu Kα X-ray beam was used to irradiate the sample, and the diffraction patterns were obtained using an imaging plate detector (BAS-IP 127 mm × 127 mm, Fuji Photo Film Co.).

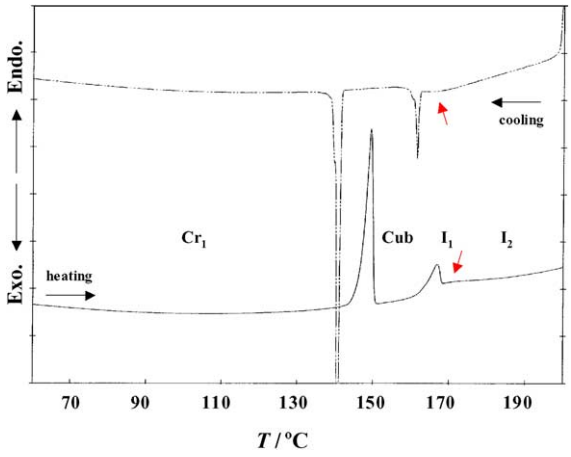

Fig. 1. DSC heating and cooling curves of EPABC. Scanning rate: 5 °C min^{-1}.

Table 1
Thermodynamic quantities associated with the phase transitions of the EPABC cubic compound

Phase transition	T (°C)	ΔH (kJ mol^{-1})	ΔS (J K^{-1} mol^{-1})	$(dt/dP)_{1\ atm}$	ΔV (cm^3 mol^{-1})
Cr → Cub	149.4	13.1	36.2	0.395_2	14.3
Cub → I	167.8	2.3	5.3	0.322_3	1.7

3. Results and discussion

3.1. Characterization under atmospheric pressure

Fig. 1 shows the DSC heating and cooling curves of EPABC sample. Two sharp peaks and a broad but small peak can be seen reversibly in the heating and cooling processes. The two sharp peaks are assigned as the Cr–Cub and Cub–I transitions in the order of increasing temperature. The cubic phase has a temperature region of about 20 °C. A broad but small peak, shown as red arrows in Fig. 1, is observed reversibly at a high temperature just above the Cub–I transition. This is attributed to the transition from the 'ordered' liquid (I_1) of dimerized molecules to the isotropic liquid (I_2) consisting of isolated molecules, already identified in ANBC(n) [8,9]. Both EPABC and ANBC(n) molecules contain carboxylic acid group at one end of molecule, which is able to form the intermolecular hydrogen bonding between the neighboring molecules in the crystalline solid and mesophase. Table 1 lists the thermodynamic quantities associated with the phase transitions of the EPABC sample.

Fig. 2 shows the POM photographs of the textures of EPABC on heating process under atmospheric pressure. The crystalline texture at 30 °C (Fig. 2a) is maintained at tempera-

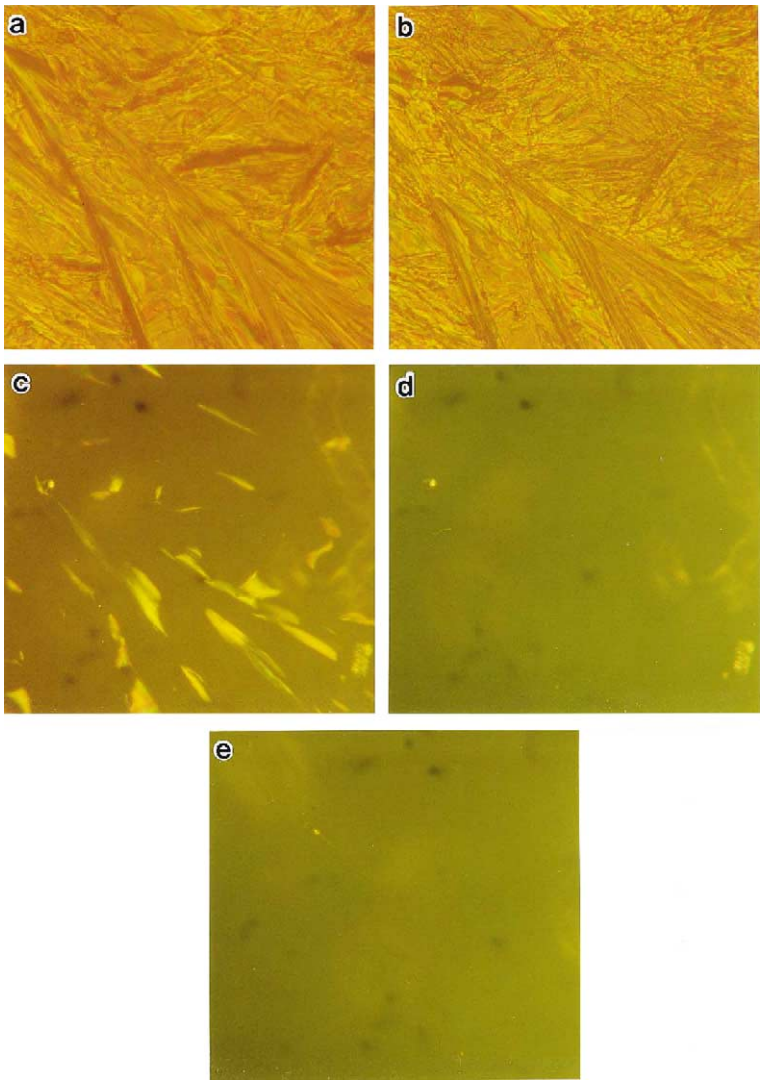

Fig. 2. POM photographs of EPABC on heating under atmospheric pressure: (a) Cr_1 at 30 °C; (b) Cr_1 at 150 °C; (c) Cr_1 → Cub transition at 152 °C; (d) Cub phase at 160 °C; and (e) isotropic liquid at 170 °C.

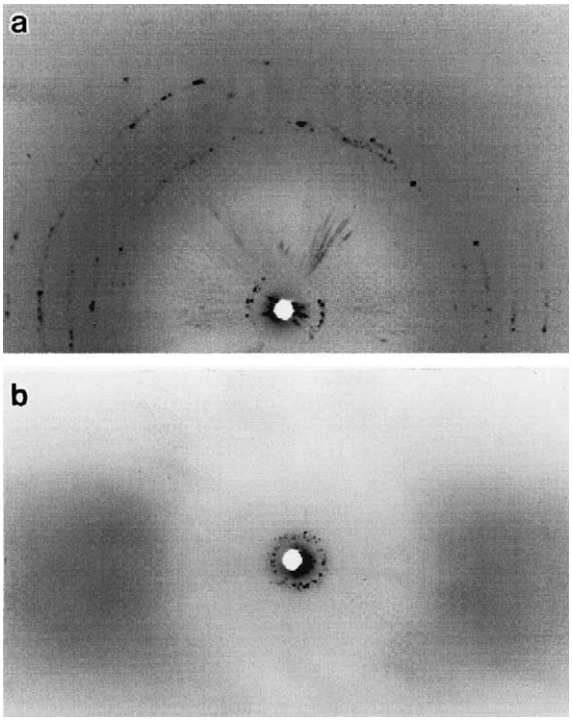

Fig. 3. X-ray diffraction patterns of the crystal and cubic phase under atmospheric pressure. (a) Cr_1 at 22 °C and (b) Cub at 155 °C.

tures up to about 150 °C (Fig. 2b). Then the crystalline texture disappears at about 152 °C (Fig. 2c). The dark field of view for the cubic phase (Fig. 2d) is held continuously at high temperatures up to 170 °C, indicating the isotropic liquid phase (Fig. 2e). On the subsequent cooling, a bright oily fluid-like texture appears rapidly at 166 °C during the I–Cub transition; and then, the texture disappears instantaneously into the black field of view for the cubic phase, as already reported by Niori et al. [14]. The oily texture appears as a monotropic phase, characteristic of a metastable phase. But the corresponding thermal transition is not observed on the DSC cooling curve. The cubic phase is confirmed to appear reversibly by the DSC and POM observations. Fig. 3 shows the X-ray diffraction

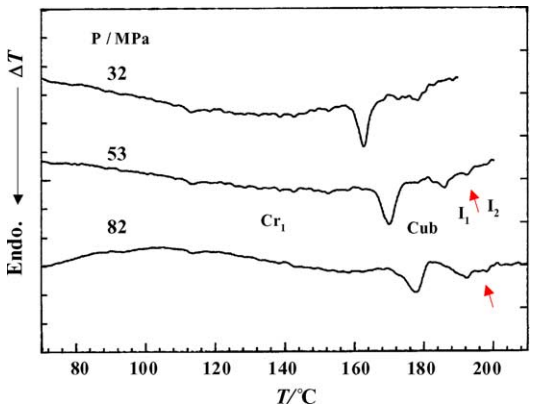

Fig. 4. DTA heating curves of EPABC at 32, 53, and 82 MPa. Heating rate: 5 °C min^{-1}.

patterns of the crystal at 22 °C and the cubic phase at 155 °C under atmospheric pressure. Both the crystalline and cubic phases show a spot-like pattern, indicating a single crystal-like structure in the solid and a polydomain structure for the cubic phase, respectively. The structural pattern of the cubic phase is closely resembled with that for the cubic phase of ANBC(16) with *Ia*3*d* space group. The values of *d* spacing associated with the reflection peaks for both the crystal and cubic phase are listed in Table 2. Many spots for the cubic phase are distributed at $2\theta = 2.63°$ ($d = 33.5$ Å) and $2\theta = 2.95°$ ($d = 29.9$ Å), which are corresponded to the (2 1 1) and (2 2 0) reflections of the cubic structure with *Ia*3*d* space group.

3.2. Thermal behavior under pressure

The thermal behavior and phase stability of the cubic phase for EPABC was investigated under hydrostatic pressures up to 300 MPa. Fig. 4 shows the DTA heating curves of the sample at 32, 53, and 82 MPa. All the heating curves show the main peak of Cr–Cub transition and a small peak of the Cub–I_1 transition at high temperature, respectively. Another small peak is often observed at a high temperature above the Cub–I_1 transition point (indicated as red arrows on the

Table 2
d spacing (Å)/2θ (°) of the reflections associated with the crystalline and cubic phases of the EPABC samples observed at various conditions

Cr_1 (1 atm, 22 °C)	Cr_2 (300 MPa, 201 °C)	Cub (1 atm, 155 °C)	Cub (50 MPa, 172 °C)
		33.5/2.63	33.2/2.66
		31.5/2.80	
		29.9/2.95	
24.3/3.63			
22.3/3.97			
	20.7/4.27		
5.2/16.9			
4.5/19.8			
4.4/20.0			
3.9/22.9			
3.6/24.9	3.8/23.6		
3.5/25.4	3.56/25.0		
3.2/28.0	3.3/27.2		

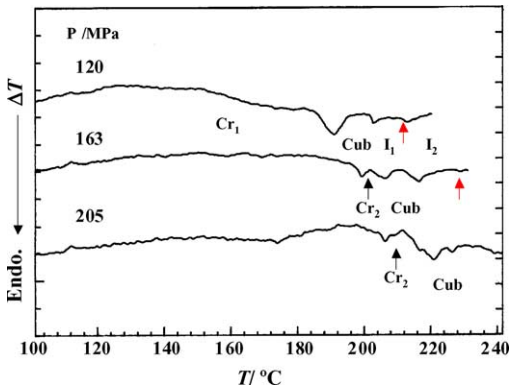

Fig. 5. DTA heating curves of EPABC at 120, 163, and 205 MPa. Heating rate: 5 °C min^{-1}.

curves at 53 and 82 MPa), indicating the I_1–I_2 transition for the dissociation of the dimerized molecule into an isolated one. Since the baselines of the DTA curves are noisy with a low S/N ratio, the quantitative analyses of the transitions were skipped in this study. Fig. 5 shows the DTA heating curves of the sample at 120, 163 and 205 MPa. The main peak of the Cr–Cub transition splits into two peaks at 163 and 205 MPa, indicating the formation of a crystalline polymorph between the normal crystal (Cr_1) and the Cub phases under high pressures. The pressure-induced crystalline polymorph is named here as Cr_2. At the same time, it is interesting to note that the temperature region of the cubic phase decreases gradually with increasing pressure. The peak temperatures of all the transitions of EPABC are plotted as a function of pressure up to 300 MPa. Fig. 6 shows the T versus P phase diagram of EPABC. The transition curves can be expressed approximately as either first or second order polynomials in terms of pressure as follows:

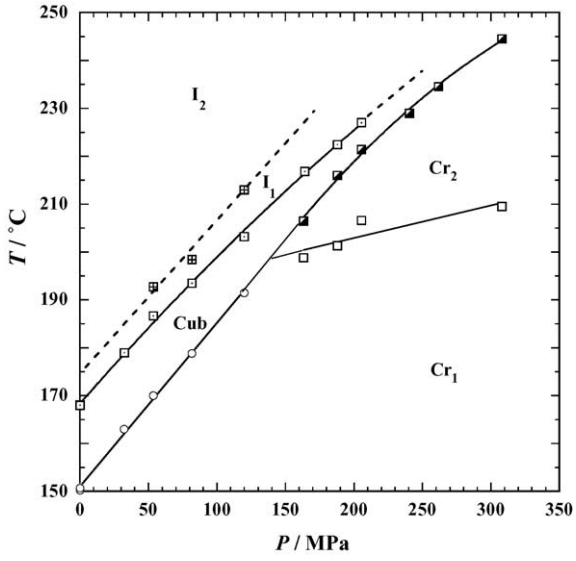

Fig. 6. Temperature vs. pressure phase diagram of EPABC constructed in the heating mode.

Transition	Peak temperature (T, °C)
$0 < P <$ ca. 140 MPa	
$Cr_1 \rightarrow$ Cub	$151.0 + 0.341_5$ (P, MPa)
ca. 140 MPa $< P$	
$Cr_1 \rightarrow Cr_2$	$189.3 + 0.068_2$ (P, MPa)
$Cr_2 \rightarrow$ Cub	$138.0 + 0.514_8$ (P, MPa) $- 5.521_3 \times 10^{-4}$ (P, MPa)^2
Whole pressures	
Cub $\rightarrow I_1$	$168.4 + 0.326_3$ (P, MPa) $- 2.041_9 \times 10^{-4}$ (P, MPa)^2
$I_1 \rightarrow I_2$	$175.0 + 0.309_7$ (P, MPa)

A triple point for the Cr_1, Cr_2, and Cub phases can be seen at about 140 MPa, 199 °C, indicating the lower limit of pressure for the formation of the Cr_2 polymorph. It is clear that the cubic phase is stable in the whole pressure region up to 300 MPa, although the temperature region decreases gradually with increasing pressure. From the thermodynamic data in Table 1 and the (dT/dP) obtained by high-pressure DTA, the volume changes at the phase transitions can be discussed qualitatively using the Clausius–Clapeyron equation $dT/dP = \Delta V/\Delta S = T\Delta V/\Delta H$. Since the Cr–Cub and Cub–I transitions have both positive values of slope dT/dP and enthalpy of transition ΔH, the volume changes are assigned to be positive. So, the cubic phase of EPABC is a thermodynamically stable phase between the crystalline and isotropic liquid phases under all pressures observed. It can be said that the cubic phase of EPABC has a common trend of destabilization with increasing pressure, as already seen in ANBC(n) system [9,11], because the temperature region for the cubic phase decreases with increasing pressure.

3.3. Morphological and structural observations under pressure

Fig. 7 shows the POM textures of the sample on heating process at 100 MPa. The crystalline texture is maintained at high temperatures up to about 180 °C (Fig. 7a). When the sample is heated, the crystalline texture changes to the dark brown field of view for the cubic phase at 183 °C (Fig. 7b), indicating the Cr → Cub transition at 100 MPa. The morphological change is corresponded well to the thermal transition observed with the high-pressure DTA. The dark field of view (Fig. 7c) for the cubic phase is held at high temperatures over the Cub–I transition (Fig. 7d). It is substantiated morphologically that the cubic phase is stable between the crystalline phase and isotropic liquid under elevated pressures. Also the X-ray pattern for the cubic phase was confirmed at 172 °C and 50 MPa. The X-ray pattern shows several weak spots on a circle with a radius of $2\theta = 2.65°$ ($d = 33.2$ Å), which can be identified as the (2 1 1) reflection of the cu-

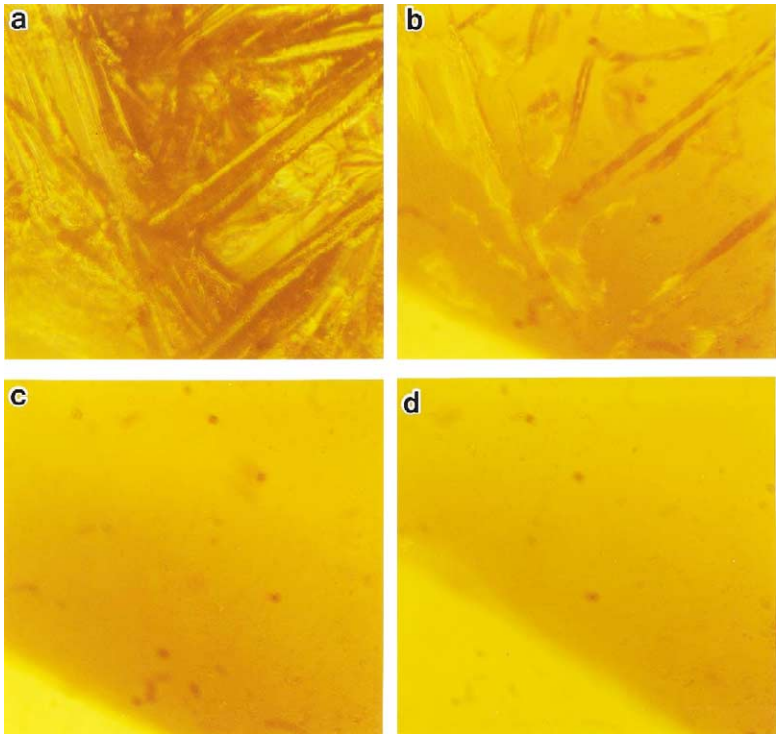

Fig. 7. POM photographs of EPABC on heating at 100 MPa: (a) Cr_1 at 180 °C; (b) Cr1 → Cub transition at 183 °C; (c) Cub phase at 184 °C; and (d) isotropic liquid at 200 °C.

bic structure. The same X-ray pattern for the cubic phase was observed at other low pressures, but the X-ray patterns at pressures above 100 MPa was ambiguously observed due to very weak reflections. At present the cubic structure is confirmed experimentally under pressures below 100 MPa, using the high-pressure POM and WAXD techniques. The Cr_2 crystalline polymorph is confirmed experimentally at 300 MPa.

4. Conclusion

The transition behavior of EPABC was investigated under hydrostatic pressures up to 300 MPa using a high-pressure DTA, a polarizing optical microscope and the WAXD apparatus equipped with a high-pressure cell. The temperature versus pressure phase diagram was constructed. It was found that the cubic phase is stable in the whole pressure region observed. At the same time the cubic phase has the common trend of destabilization with increasing pressure because its temperature range decreases gradually with increasing pressure. The transition sequence of Cr–Cub–I observed at atmospheric pressure, is held in the whole pressure region. A crystalline polymorph Cr_2 is found to appear between the normal crystal Cr_1 and Cub phases under elevated pressure above about 150 MPa. The difference in stability of cubic phases should be analyzed in relation to the structure of the cubic phases

References

[1] G.W. Gray, B. Jones, F. Marson, J. Chem. Soc. Part I (1957) 393–401.
[2] S. Diele, P. Göring, in: D. Demus, J.W. Goodby, G.W. Gray, H.-W. Spiess, V. Vill (Eds.), Handbook of Liquid Crystals, vol. 2, Wiley–VCH, Weinheim, 1998, pp. 887–900.
[3] V. Luzzati, A. Spegt, Nature 215 (1967) 701–704.
[4] A. Tardieu, J. Billard, J. Phys. (Paris) Coll. 37 (1976) C3 79–81.
[5] A.-M. Levelut, Y. Fang, Colloq. Phys. 23 (1991) C7–229.
[6] A.-M. Levelut, M. Clerc, Liq. Cryst. 24 (1998) 105–115.
[7] D.S. Shankar Rao, S. Krishna Prasad, V. Prasad, S. Kumar, Phys. Rev. E 59 (1999) 5572–5576.
[8] Y. Maeda, G.-P. Cheng, S. Kutsumizu, S. Yano, Liq. Cryst. 28 (2001) 1785–1791.
[9] Y. Maeda, S. Krishna Prasad, S. Kutsumizu, S. Yano, Liq. Cryst. 30 (2003) 7–16.
[10] Y. Maeda, K. Morita, S. Kutsumizu, Liq. Cryst. 30 (2003) 157–164.
[11] Y. Maeda, K. Saito, M. Sorai, Liq. Cryst. 30 (2003) 1139–1149.
[12] Y. Maeda, T. Ito, S. Kutsumizu, Liq. Cryst. 31 (2004) 623–632.
[13] Y. Maeda, T. Ito, S. Kutsumizu, Liq. Cryst. 31 (2004) 807–820.
[14] T. Niori, J. Yamamoto, H. Yokoyama, Mol. Cryst. Liq. Cryst. 364 (2001) 843–850.
[15] Y. Maeda, H. Kanetsuna, K. Nagata, K. Matsushige, T. Takemura, J. Polym. Sci. Polym. Phys. Ed. 19 (1981) 1313–1324;
Y. Maeda, H. Kanetsuna, K. Tagashira, T. Takemura, J. Polym. Sci. Polym. Phys. Ed. 19 (1981) 1325–1331;
Y. Maeda, H. Kanetsuna, Bull. Res. Inst. Polym. Tex. 149 (1985) 119–125;
Y. Maeda, Thermochim. Acta 163 (1990) 211–218.
[16] Y. Maeda, M. Koizumi, Rev. Sci. Instrum. 67 (1996) 2030–2031;
Y. Maeda, M. Koizumi, Rev. High Pressure Sci. Technol. 7 (1998) 1532–1533.